Proceedings of International Structural Engineering and Construction, 10(1), 2023
Innovative Theory and Practices in Structural Engineering and Construction
Edited by Karatas, A., Iranmanesh, A., Gurgun, A., Yazdani, S., and Singh, A.

ISSN: 2644-108X
www.doi.org/10.14455/ISEC.2023.10(1).STR-03

SPECIFIC BENDING STIFFNESS COMPARISON OF SPHERICALLY VOIDED BIAXIAL CONCRETE SLABS AND SOLID SLABS

GIRUM URGESSA and HOMA HAGHIGHI

Dept of Civil, Environmental and Infrastructure Engineering, George Mason University, Fairfax, VA, USA

Spherically hollow or voided biaxial concrete slab (SVBS) configurations that implement empty composite balls as a filling material are gaining momentum due to the reduction in mass-to-capacity and mass-to-stiffness fractions. The SVBS configuration depends on taking out the ineffective concrete mass near the mid-section of a floor in which bending stress is less. This will in turn dramatically reduce the overall structural dead weight. This paper presents comparison of normalized bending stiffnesses for a representative spherically voided biaxial concrete slab with its counterpart solid slab. A representative SVBS element is chosen for capturing the volume action (RVE). The RVE is the primary sub-unit that is periodic and it is modeled in finite element software to determine the stiffness values noting that the SVBS is macroscopically similar, elastic in the linear range, and exhibits isotropic behavior transversely with no thermal stresses. An example SVBS system is shown to be more efficient with 16% higher normalized (specific) stiffness values when compared to solid slabs of equal thicknesses.

Keywords: SVBS, RVE, Micromechanics, Flexural stiffness.

1 INTRODUCTION

In recent years, spherically voided biaxial slabs (SVBS) were extensively implemented in reinforced concrete planar diaphragms when regular solid cross-sections do not meet design criteria, including higher strength-to-mass or high stiffness-to-mass fractions. SVBS systems have considerable bending capacity because of the two uniform sections separated by a hollow empty ball. SVBS have several advantages (Marais *et al*. 2011, Teja *et al*. 2012, Casey and Urgessa 2012, Mota 2013): it provides flexible degrees of choice for architects: shape optimization, cantilever spans, wide spans, less supported decks, reduced number of columns and walls providing excellent flexibility; it allows inside building designs to be freely changed during use; it reduces the amount of concrete used leading to significant weight reduction and extended span possibilities in the order of 20 - 25 m between vertical members without the need of using beams; it allows the elimination of beams and column capitals and in essence reducing story heights; and it increases sustainability ratings (Choi *et al*. 2008, Ali *et al*. 2014a).

While several studies are reported on computational work related to standard RC slabs, more work is needed for SVBS systems. Earlier analysis approaches rely on using the empirical methods outlined for regular flat slabs and altering it to determine system responses and SVBS system capacity (Schnellenbach-Held and Pfeffer 2002). This approach is partly selected because of the challenges associate with analyzing the kinematic parameters arising from the complex form of SVBS systems. The plastic ball voids are not prismatic with discrete volumes in a 2D space (Tina

2010). Hence, the standard theory of shells and plates as well as the grillage procedure will not be able to simulate the real responses to an accurate level.

2 MICROMECHANICS

The complexity of the entire floor slab system results in heterogeneous relationships between strain and stress, which then provides difficulties for describing the SVBS structural responses adequately. The force and deflection relationship of any diaphragm is a function of its stiffness in extension, flexure, shear and torque. Structural engineers will benefit from valid analysis methods developed to address this issue. Figure 1 shows a micromechanics modelling approach that includes the geometric description of the void configurations, the SVBS component mechanical properties, and application of mechanics for determining macroscopic constitutive behavior of the SVBS system.

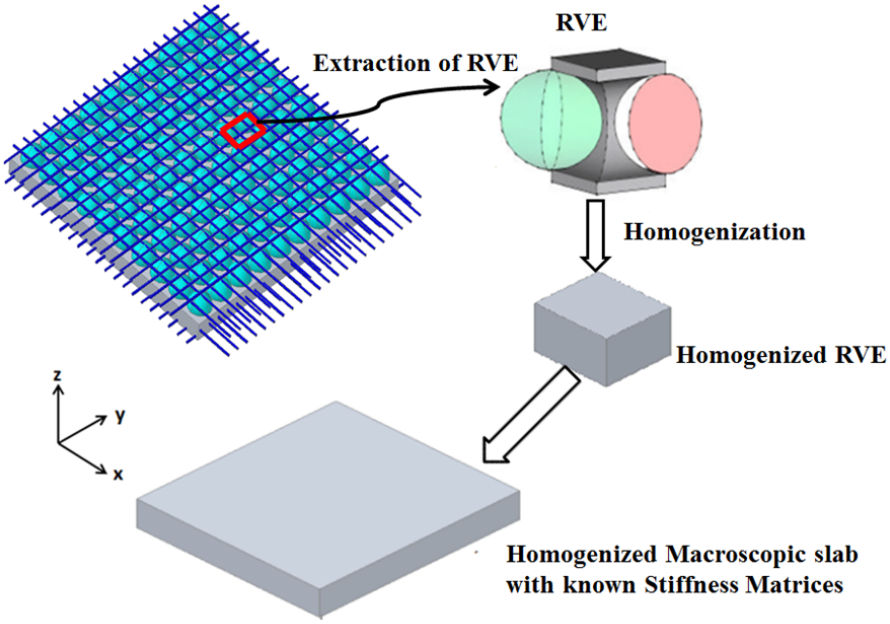

Figure 1. Homogenization.

Once the RVE is selected, it will be used to determine the relevant stiffness values of the SVBS material. Key assumed items include: the SVBS is macroscopically homogeneous, isotropic in the transverse direction, and with zero thermal stress; the reinforcement is homogeneous with equal spacing, and with 100% bond stress transfer; and the concrete is homogeneous (Urgessa *et al*. 2005, Voros 2011, Ali *et al*. 2014b, Muda *et al*. 2023). Figure 2 shows an RVE extraction scheme. The RVE describes a key part with all important components and statistical homogeneity. Therefore, the properties of the RVE can be assumed to be equivalent to the properties of the SVBS. The statistical component ensures that the sizes of the RVE, lx and ly, will meet the criteria $lx << a$ and $lz << b$, where a and b are the length and width of the SVBS.

Eqs. (1), (2) and (3) show the normal force, moment, and transverse shear relationships respectively, where ε_1, ε_2, and γ_{12}, are normal and shear strains at the middle surface; κ_1, κ_2, and κ_3 are curvatures; γ_{13} and γ_{23} are transverse shear strains.

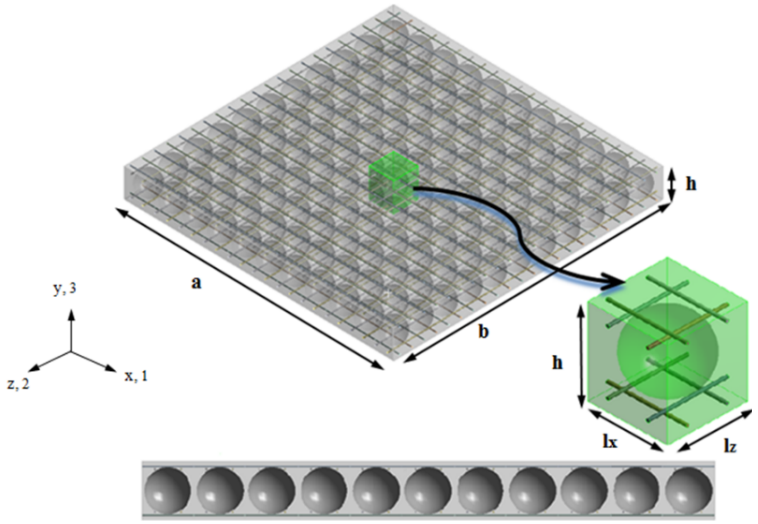

Figure 2. RVE extraction scheme.

$$\begin{Bmatrix} N_1 \\ N_2 \\ N_3 \end{Bmatrix} = \begin{bmatrix} A_{11} & A_{12} & A_{13} \\ A_{21} & A_{22} & A_{23} \\ A_{31} & A_{32} & A_{33} \end{bmatrix} \begin{Bmatrix} \varepsilon_1 \\ \varepsilon_2 \\ \gamma_{12} \end{Bmatrix} + \begin{bmatrix} B_{11} & B_{12} & B_{13} \\ B_{21} & B_{22} & B_{23} \\ B_{31} & B_{32} & B_{33} \end{bmatrix} \begin{Bmatrix} \kappa_1 \\ \kappa_2 \\ \kappa_3 \end{Bmatrix} \tag{1}$$

$$\begin{Bmatrix} M_1 \\ M_2 \\ M_3 \end{Bmatrix} = \begin{bmatrix} B_{11} & B_{12} & B_{13} \\ B_{21} & B_{22} & B_{23} \\ B_{31} & B_{32} & B_{33} \end{bmatrix} \begin{Bmatrix} \varepsilon_1 \\ \varepsilon_2 \\ \gamma_{12} \end{Bmatrix} + \begin{bmatrix} D_{11} & D_{12} & D_{13} \\ D_{21} & D_{22} & D_{23} \\ D_{31} & D_{32} & D_{33} \end{bmatrix} \begin{Bmatrix} \kappa_1 \\ \kappa_2 \\ \kappa_3 \end{Bmatrix} \tag{2}$$

$$\begin{Bmatrix} Q_1 \\ Q_2 \end{Bmatrix} = \begin{bmatrix} E_{55} & 0 \\ 0 & E_{66} \end{bmatrix} \begin{Bmatrix} \gamma_{13} \\ \gamma_{23} \end{Bmatrix} \tag{3}$$

where, N_1, N_2, and N_3 are the normal and shear forces per unit width, M_1, M_2 are the bending moments per unit width in the x and z directions respectively, M_3 is the twisting moment per unit width and Q_1, Q_2 are the transverse shear forces per unit width. The stiffness matrices are collectively called the ABDE matrix.

3 EXAMPLE SVBS - BUBBLEDECK

The BD230 SVBS from BubbleDeck was used for a comparative study with its counterpart solid slab. Table 1 shows the properties of BD230.

Table 1. Geometric parameters of SVBS230.

Thickness (mm)	230
Hollow Diameter (mm)	180
Length (mm)	210
Width (mm)	210
Hollow Diameter/Thickness	180/230
Mass (kg)	16.31
Reinforcing Steel No. & Size	4#4
Concrete Cover (mm)	30

4 DETERMINATION OF FLEXURAL STIFFNESS, D

To provide an illustration, the bending stiffness D is determined by applying unit values to each angle component while simultaneously holding aa other kinematic parts to zero through required

constraints. Following that, the moments are determined from the locations of zero stress in the depth. The same procedure is followed in mutually perpendicular sides. Determining D_{11} and D_{21} of the system requires implementation of a rigid support scenario at the origin of the side face and a rotation of unit value, $\kappa_2 = 1$ rad, is applied at the extreme side of $x = lx$ through ANSYS's farther node deflection tool capability (Kohnke 1982). This provides for both displacements and rotations to be acted upon at a random orientation. The default place is always the geometric center. Figure 3 shows the addition of displacement scenarios on y-z plane at faces $z = 0$ and $z = lz$. The z-direction displacement is fixed at the lateral faces at $z = 0$ and $z = lz$. With a similar approach, the A, B, D, and E matrices of any SVBS can be determined.

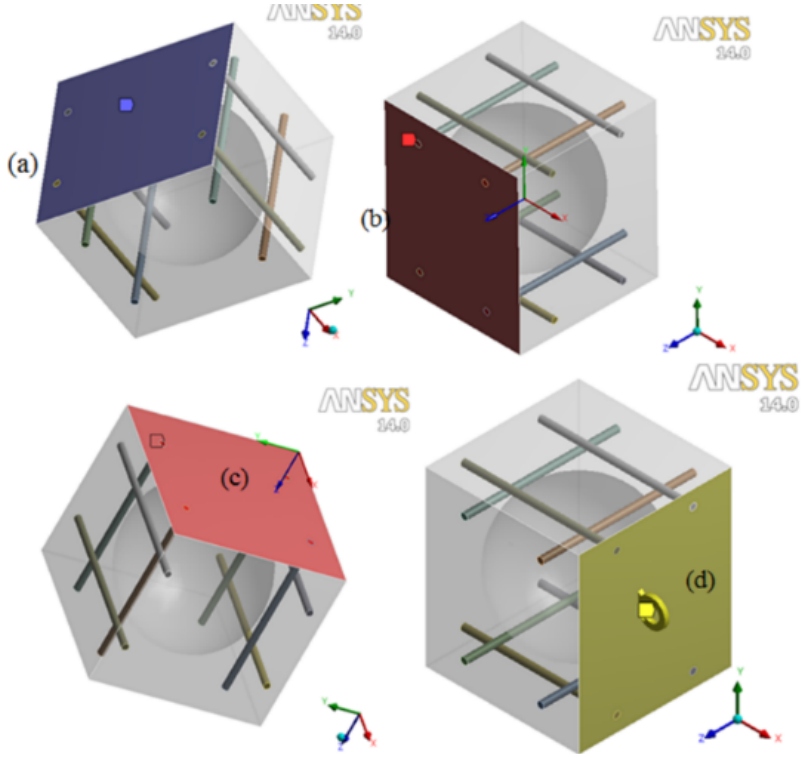

Figure 3. Boundary conditions (BC) applied: (a) the face with fixed BC, (b) and (c) the faces with zero displacement only in z-directions, and (d) the face with rotation of 1 rad applied about the z-axis.

5 COMPARISION BETWEEN SOLID AND SVBS SLABS OF EQUAL THICKNESS

The BD230 SVBS from BubbleDeck was used for a comparative study with its counterpart solid slab. Table 1 shows the calculated ABDE matrix entries. In this study, the SVBS 230 and SOLID 230 concrete mixes were assumed to be the same. Optimal mixes can be determined from established methods (Kim *et al*. 2019, Tahmouresi *et al*. 2021). As shown in Tables 2 and 3 and as expected, the SVBS stiffness are ususally on the lower end when compared to their counterpart solid slabs.

More importantly, the shear and tensile SVBS stiffness values are lower by a significant margin. We conclude that SVBS systems may not safe and cost effective for conditions that result in higher shear or axial stresses. On the contrary, if the specific stiffness values are calculated by the ration of the stiffness to the mass of the slab systems, the benefit of SVBS in flexural bending will be observed.

Table 2. Material properties of SVBS230 and SOLID230.

Parameters	SVBS230	SOLID230	Ratio, %
Geometry			
Thickness (mm)	230	230	-
Hollow Former Diameter (mm)	180	-	-
Length (mm)	210	210	-
Width (mm)	210	210	-
Hollow Diameter/Thickness	180/230	-	-
Mass (kg)	16.31	23.33	69.89
Reinforcement No. & Size	4#4	4#4	-
Concrete Cover (mm)	30	30	-
Stiffness Matrix Entries			
A_{11} (N/mm)	4.60E+06	7.83E+06	58.76
A_{12} (N/mm)	6.77E+05	1.57E+06	43.20
A_{33} (N/mm)	1.18E+06	2.76E+06	42.91
D_{11} (N-mm)	3.51E+10	4.19E+10	83.83
D_{21} (N-mm)	6.95E+09	8.73E+09	79.69
D_{33} (N-mm)	1.72E+10	2.14E+10	80.07
E_{55} (N/mm)	1.92E+06	3.81E+06	50.46

D_{11} represents the significant flexural stiffness. Since standard slabs are mainly loaded in-plane, their resistance is determined from flexure. Table 2 shows that SVBS230 is significantly better and effective in flexure than standard slabs having the same depth with an approximately 17% margin. Assuming the same density of concrete, a higher flexural capacity is obtained from SVBS systems when normalized by weight.

Table 3. Specific stiffness values of SVBS230 and SOLID230 slabs.

Slab Type	Specific Stiffness (normalized by mass)						
	A_{11} N/mm/kg	A_{12} N/mm/kg	A_{13} N/mm/kg	D_{11} N-mm/kg	D_{21} N-mm/kg	D_{33} N-mm/kg	E_{55} N/mm/kg
SVBS230	2.82E+05	4.15E+04	7.25E+04	2.15E+09	4.26E+08	1.05E+09	1.18E+05
SOLID230	3.36E+05	6.72E+04	1.18E+05	1.79E+09	3.74E+08	9.18E+08	1.63E+05
% Diff.	-18.94	-61.80	-62.90	16.63	12.29	12.70	-38.52

6 CONCLUSIONS

This paper presents comparison of normalized (specific) bending stiffnesses for a representative spherically voided biaxial concrete slab and its counterpart solid slabs with the same thickness. A periodic element of SVBS serves as a representative volume element (RVE). The RVE is then modeled numerically to calculate the stiffness coefficients with the assumption that the SVBS is macroscopically homogeneous, linearly elastic, and transversely isotropic with no thermal stress. An example system, SVBS230, was shown to be more efficient with 17% higher specific stiffness values when compared to SOLID230 of equal thicknesses.

Acknowledgements

This research was supported by George Mason University. The authors are grateful for this support.

References

Ali, W. B., and Urgessa, G. S., *Structural Capacities of Spherically Voided Biaxial Slab (SVBS),* Proceedings of Structures Congress 2014, ASCE, 785-796, Boston, Massachusetts, April 3-5, 2014a.

Ali, W., and Urgessa, G., *Computational Model for Internal Relative Humidity Distributions in Concrete*, Journal of Computational Engineering, Hindawi, 2014, 539850, March, 2014b.

Casey, M. J., and Urgessa, G. S., *Rebar Cage Construction and Safety: Best Practices*, American Society of Civil Engineers (ASCE), 2012.

Choi, K. K., Urgessa, G., Taha, M. M., and Maji, A. K., *Quasi-balanced Failure Approach for Evaluating Moment Capacity of FRP Underreinforced Concrete Beams,* Journal of Composites for Construction, ASCE, 12(3), 236-245, June, 2008.

Kim, D., Kim, C. Y., Urgessa, G., Choi, J. H., Park, C., and Yeon, J. H., *Durability and Rheological Characteristics of High-volume Ground-granulated Blast-furnace Slag Concrete Containing $CaCO_3$/Anhydrate-based Alkali Activator*, Construction and Building Materials, Elsevier, 204, 10-19, April, 2019.

Kohnke, P. C., *ANSYS,* Springer-Verlag, Heidelberg, Berlin, 1982.

Marais, C. C., Robberts, J. M., and Van Rensburg, B. W. J., *Spherical Void Formers in Concrete Slabs: Technical Paper*, Journal of the South African Institution of Civil Engineering, South African Institution of Civil Engineering (SAICE), 53(1), 2-11, January, 2011.

Mota, M., *Voided "Two-Way" Flat Slabs*, Proceedings of the Structures Congress 2013, ASCE, 1640-1649, Pittsburgh, Pennsylvania, May 2-4, 2013.

Muda, M. M., Legese, A. M., Urgessa, G., and Boja, T., *Strength, Porosity and Permeability Properties of Porous Concrete Made from Recycled Concrete Aggregates*, Construction Materials, MDPI, 3(1), 81-92, March, 2023.

Schnellenbach-Held, M., and Pfeffer, K., *Punching Behavior of Biaxial Hollow Slabs*, Cement and Concrete Composites, Elsevier, 24(6), 551-556, December, 2002.

Tahmouresi, A., Robati, A., Urgessa, G., and Haghighi, H., *A Combined Genetic Algorithm-Artificial Neural Network Optimization Method for Mix Design of Self Consolidating Concrete*, International Journal of Structural and Civil Engineering Research, 10(3), 106-112, August, 2021.

Teja, P. P., Kumar, P. V., Anusha, S., Mounika, C. H., and Saha, P., *Structural Behavior of Bubble Deck Slab*, Proceedings of IEEE-International Conference on Advances in Engineering, Science and Management (ICAESM-2012), IEEE, 383-388, Bangalore, India, November 28-29, 2012.

Tina, L., *Structural Behavior of BubbleDeck® Slabs and Their Application to Lightweight Bridge Decks*, Master's Thesis, Department of Civil and Environmental Engineering, Massachusetts Institute of Technology, USA, 2010.

Urgessa, G., Horton, S., Taha, M. M. R., and Maji, A., *Significance of Stress-block Parameters on the Moment Capacity of Sections Under-reinforced with FRP*, International Concrete Abstracts Portal, SP-230-87, 1531-1550, October, 2005.

Voros, S., *Analysis of Bi-axial Hollow Core Slabs*, Proceedings of the 13th Professional Conference on Postgraduate Students (JUNIORSTAV 2011), Brno University of Technology, Czech Republic, 2011.